Supporting information for: Supplement to 'CO-induced Smoluchowski ripening of Pt-cluster arrays on the graphene/Ir(111) moiré'

Timm Gerber,[*,†] Jan Knudsen,[‡,¶] Peter J. Feibelman,[§] Elin Grånäs,[‡] Patrick Stratmann,[†] Karina Schulte,[¶] Jesper N. Andersen,[‡,¶] and Thomas Michely[†]

II. Physikalisches Institut, Universität zu Köln, Zülpicher Str. 77, 50937 Köln, Germany, Division of Synchrotron Radiation Research, Lund University, Box 118, 22 100 Lund, Sweden, MAX IV Laboratory, Lund University, Box 118, 22 100 Lund, Sweden, and Sandia National Laboratories, Albuquerque, New Mexico 87185-1415, USA

E-mail: gerber@ph2.uni-koeln.de

Movies of CO-induced Pt-cluster diffusion and coalescence

In the drift corrected STM movies the exposure to CO is indicated by a white frame and the label "CO". The STM tip was retracted when the CO valve was opened or closed giving rise to a partially blank image. A tunneling voltage of 1 V and low tunneling currents in the range from 32 pA to 52 pA were used in order to avoid tip-cluster interaction. The frame size is always 600 Å $\times$ 600 Å.

[*]To whom correspondence should be addressed
[†]II. Physikalisches Institut, Universität zu Köln, Zülpicher Str. 77, 50937 Köln, Germany
[‡]Division of Synchrotron Radiation Research, Lund University, Box 118, 22 100 Lund, Sweden
[¶]MAX IV Laboratory, Lund University, Box 118, 22 100 Lund, Sweden
[§]Sandia National Laboratories, Albuquerque, New Mexico 87185-1415, USA

Movie 1

$\theta = 0.05$ ML Pt. The experimental recording time is $t_{\text{experiment}} = 10200$ s, the movie playtime in regular speed $t_{\text{movie}} = 38$ s and the total number of frames $N = 194$. The applied CO pressure was $p_{\text{CO}} = 1 \times 10^{-9}$ mbar, the tunneling current was $I = 44$ pA. Two doses of CO of 0.4 L and 0.7 L were given, in total 1.1 L CO.

Movie 2

$\theta = 0.20$ ML Pt, $t_{\text{experiment}} = 5220$ s, $t_{\text{movie}} = 19$ s, $N = 98$, $p_{\text{CO}} = 1 \times 10^{-8}$ mbar, $I = 49$ pA. Two doses of CO of 8 L each were given, in total 16 L CO.

Movie 3

$\theta = 0.44$ ML Pt, $t_{\text{experiment}} = 3360$ s, $t_{\text{movie}} = 12$ s, $p_{\text{CO}} = 1 \times 10^{-8}$ mbar, $N = 65$, $I = 52$ pA. After start CO was dosed continuously till the end of the movie, total dose 20 L.

Movie 4

$\theta = 0.05$ ML Pt, $t_{\text{experiment}} = 11580$ s, $t_{\text{movie}} = 43$ s, $N = 219$, $p_{\text{CO}} = 1 \times 10^{-9}$ mbar, $I = 32$ pA. After start CO was dosed continuously till the end of the movie, total dose 9 L.

Relevance of tip-cluster interactions

As pointed out in the main manuscript, tip-cluster interaction could not entirely be avoided during image acquisition. We carefully established that tip-cluster interaction decreases monotonically with the tunneling resistance, i.e. lowering the tunneling current and increasing the tunneling voltage both reduce the probability of tip-cluster interaction. The tunneling parameters chosen ($U = 1$ V and $I = 32 - 52$ pA) are a trade-off between minimizing tip-cluster interaction on the one hand and maintaining a reasonable lateral resolution plus speed of the feedback loop for time resolution of the processes on the other hand.

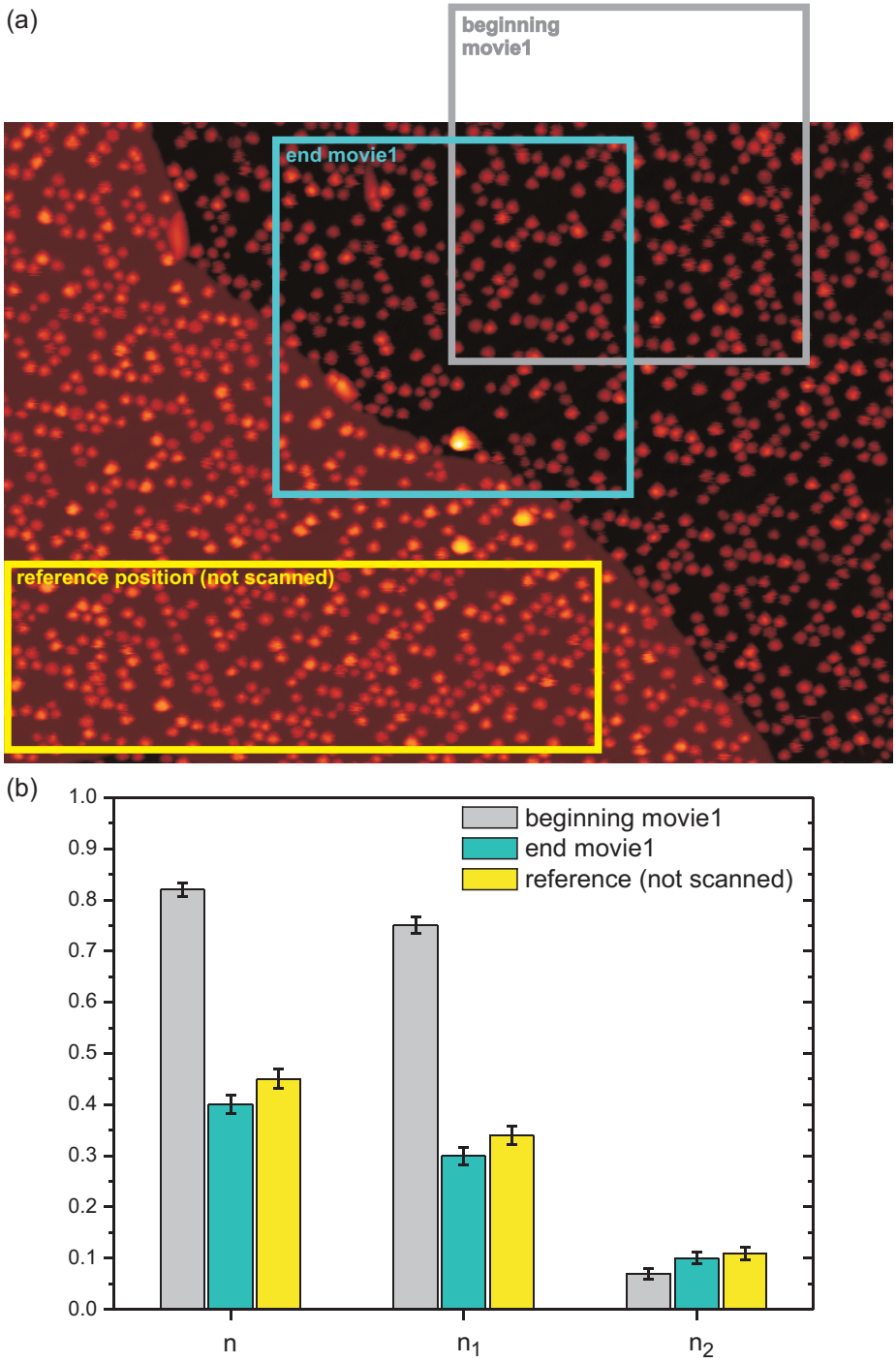

Figure 1: (a) 0.05 ML Pt cluster array imaged after movie 1 was recorded and sintering had ceased. The boxes mark the positions of the first frame of movie 1 (gray), of the last frame of movie 1 (blue) as well as a location of the sample not scanned before (yellow). Image size is 1400Å $\times$ 1000Å. (b) Corresponding filling factors n_1, n_2 and n of the clusters in the regions marked in (a).

Careful image-by-image analysis of movies 1-4 provides evidence for cluster pick-up and rare events of material deposition. Also cluster motion to another moiré unit cell and cluster height changes are observed while the tip is scanning the respective clusters. However, since cluster motion and cluster height changes are frequent in the related coverage regimes, such events must take place occasionally when the tip is just scanning the cluster under concern and need not to be due to a tip-cluster interaction.

In order to settle this issue, Figure 1 provides a quantitative analysis for an 0.05 ML cluster array related to the experiment of movie 1. Small clusters, as here with an initial $s_{av} = 5$, are least strongly bound and therefore most susceptible to tip-cluster interaction. Figure 1(a) displays a large scale topograph, in which the locations of the first frame of movie 1 (gray square) and the last frame of movie 1 (blue square) have been indicated. In between the squares the image frame gently drifted from frame to frame. The lower part of the topograph has not been scanned before, the left part only once, prior to CO exposure. It is apparent that close to the step edge in the scanned area (blue square) n is somewhat lower and an extraordinary large cluster is present. These facts are indeed related to tip-cluster interaction. However, the other area in the blue square and its surrounding display very similar appearance and filling factors. Figure 1(b) provides a bar chart, where n_1, n_2 and n are compared before CO exposure [gray bar, evaluated from area of gray square in Figure 1(a)], after CO exposure in the last frame of movie 1 [blue bar, evaluated from blue square in Figure 2(a)] and after CO exposure in an area never scanned before [yellow bar, evaluated from yellow rectangle in Figure 1(a)]. In total, the filling factor decreased from $n = 0.82$ before CO exposure to $n = 0.40$ in the continuously scanned area as compared to $n = 0.45$ in the area never scanned before. Though there is a small and noticeable tip-cluster interaction effect, based on this analysis it must be concluded that the STM movies provide a proper qualitative view of CO adsorption induced dynamic effects in the cluster arrays.

In support of this conclusion, Figure 2 displays side-by-side the same location prior to CO exposure [Figure 2(a)] and after clustering sintering had ceased [Figure 2(b)]. The location has not been scanned in between. Figure 2(b) is indeed the upper left corner of Figure 1(a). Qualita-

tively and quantitatively it displays the same changes as shown in Fig. 1(a) and 1(b) of the main manuscript and as apparent from movie 1.

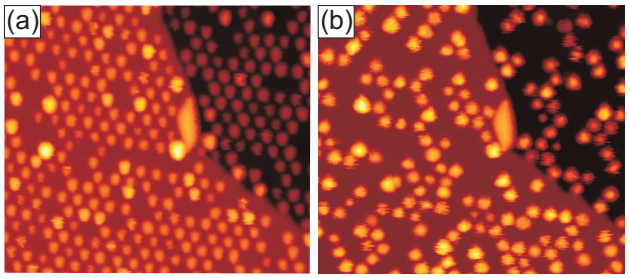

Figure 2: 0.05 ML Pt cluster array imaged (a) before and (b) after movie 1 was recorded (thus before and long time after CO exposure), but not imaged in between. Image size is 460Å x 400Å.

C1 s XPS spectra for 0.20 ML and 0.44 ML Pt cluster arrays

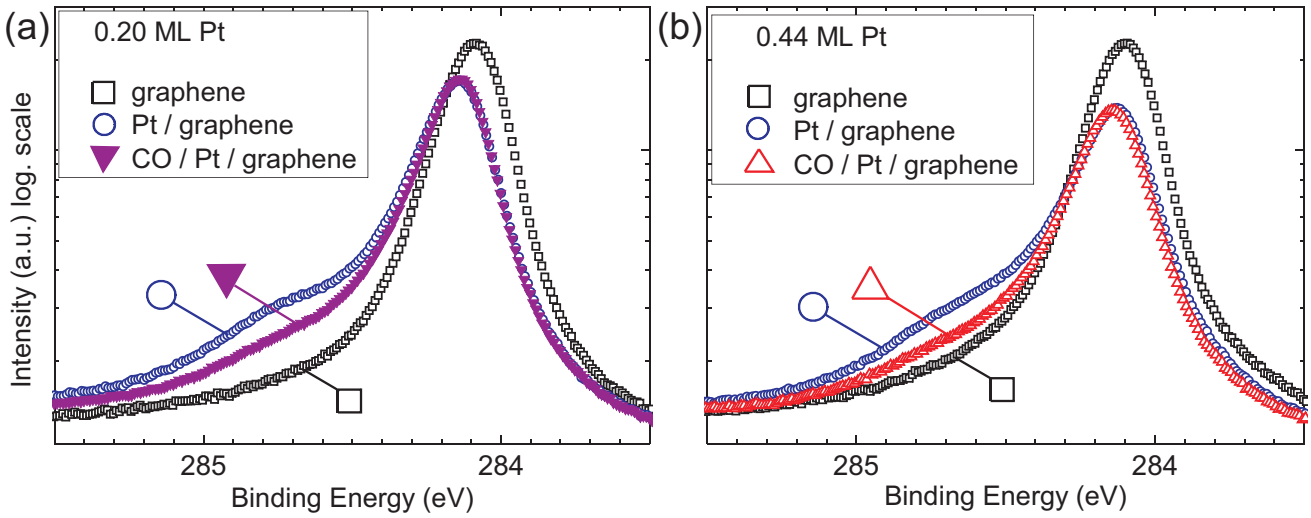

Figure 3: C 1s spectra of pristine Gr/Ir(111) (open black squares), Gr/Ir(111) with Pt-cluster array (open blue circles) and of Gr/Ir(111) with Pt cluster array after exposure to 10 L CO at 300 K (triangles). (a) 0.20 ML Pt cluster array, (b) 0.44 ML Pt cluster array.

Figure 3(a) and (b) display the C 1s region of Gr/Ir(111) before (open black squares) and after (open blue circles) room temperature deposition of 0.20 ML Pt and 0.44 ML Pt, respectively. For Gr/Ir(111) the spectrum is fitted with a single C 1s peak located at 284.1 eV with a full width at half maximum (FWHM) of 0.22 eV. The Pt deposition is associated with the development of a

broad shoulder in the binding energy range of 284.3 - 285 eV. The shoulder is linked to a local rehybridization of graphene in the vicinity and below the clusters as discussed in the main text. In addition, shifts of the main peak towards higher binding energy are observed, which we assign to doping by the Pt-clusters.[1] After exposing the cluster arrays to 10 L CO the rehybridization shoulder diminishes, as for the 0.05 ML case discussed in the main text. This is shown by the C 1s spectra represented by triangles in Figure 3(a) and (b). Distinct to the 0.05 ML case, the C 1s peak does not shift back to its original position.

Intensity of the rehybridization shoulder

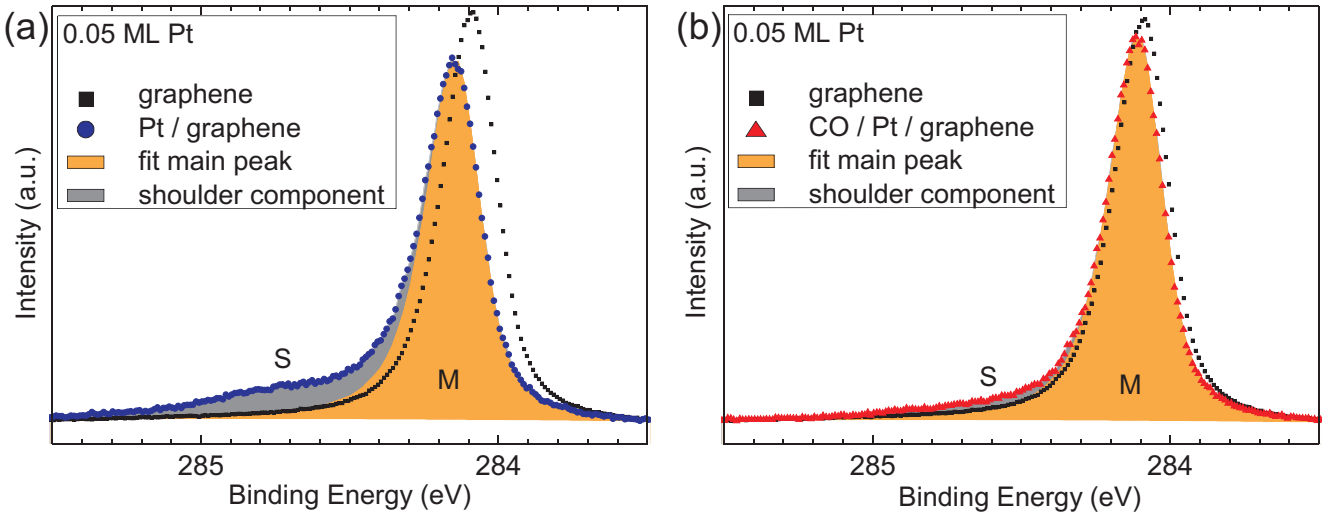

Figure 4: Spectra and fitted components visualizing the shoulder intensity and the shift of the main graphene peak as displayed in Figure 2(e) of the manuscript (see text). (a) C 1s spectrum of pristine Gr/Ir(111) (full black squares) and after deposition of 0.05 ML Pt full blue circles). (b) C 1s spectrum of pristine Gr/Ir(111) (full black squares) and after Pt deposition followed by exposure to 5 L (full red triangles).

Figure 4 (a) and (b) show how the intensity of the rehybridization shoulder and the shift of the main peak in Figure 2(e) of our manuscript were obtained. Figure 4 (a) displays a C 1s spectrum of clean graphene (full black squares) and after deposition of 0.05 ML Pt (full blue circles, corresponds to first data point in Figure 2(e)). After Pt deposition the main peak is fitted with a single component [orange area in Figure 4(a)] of the same shape and width as used for the C 1s peak of

clean graphene. The shoulder intensity [gray area in Figure 4(a)] is then estimated as the difference between the spectrum after Pt deposition and the main, orange component.

Figure 4 (b) displays the C 1s spectrum for clean graphene (full squares) and after CO exposure of the 0.05 ML Pt particles [full red triangles, corresponds to last data point in Figure 2(e)]. The shoulder intensity is again estimated as the difference between the spectrum after CO exposure and the main, orange component.

The core level shift is always given as the difference of the position of the original C 1s graphene peak position at 284.1 eV and the position of the fitted main, orange component.

References

1. Knudsen, J.; Feibelman, P. J.; Gerber, T.; Grånäs, E.; Schulte, K.; Stratmann, P.; Andersen, J. N.; Michely, T. Clusters Binding to the Graphene Moiré on Ir(111): X-ray Photoemission Compared to Density Functional Calculations. *Phys. Rev. B* **2012**, *85*, 035407.